**Pluto and Charon's Topographic Variance Spectra from Limb Profiles.** J. W. Conrad[1], F. Nimmo[1], R. A. Beyer[2,3], P. M. Schenk[4], and C. J. Bierson[1], [1]Dept. Earth and Planetary Sciences, University of California Santa Cruz, Santa Cruz, CA 95064, USA. (jwconrad@ucsc.edu) [2]NASA Ames. [3]Sagan Center at the SETI Inst. [4]Lunar and Planetary Inst.

**Introduction:** The New Horizons mission [1] revealed Pluto as a geologically active body [2,3] while Charon's surface is older but also tectonically deformed [4]. Topography can be used to probe the geophysics of these bodies, and can be derived either from stereo observations [5,6] or from limb profiles [7]. In this work we focus on limb profiles and look at the variation of topographic roughness with wavelength to make geophysical inferences [8].

**Topography:** To derive topography from limb profiles we first locate the limb in an image using Method A from [7]. Then an orthographic projection [9] is used in conjunction with spacecraft location and pointing information to determine the latitude, longitude and radius at each limb location. In Figure 1 we present maps of Pluto and Charon which show limb topography locations and values. Profiles are temporally positioned from right to left in the approach sequence.

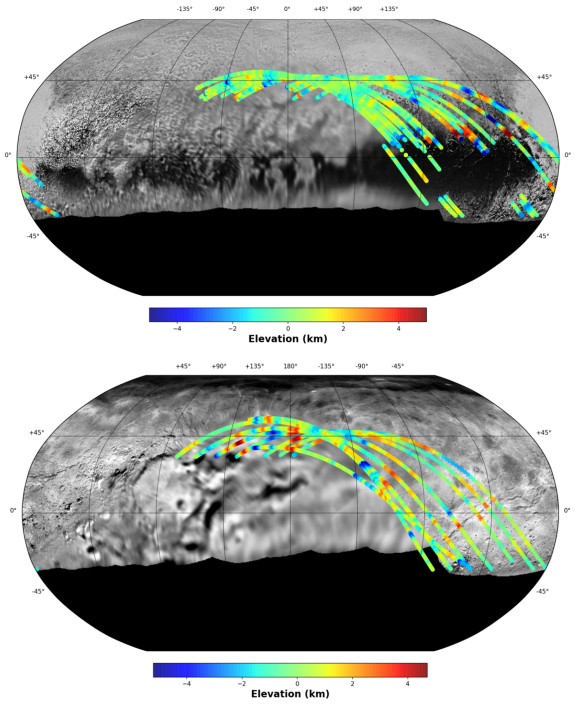


**Figure 1:** Top: Albedo map of Pluto with limb profile topography overlain. Centered on the Charon-facing/"Far" side. Bottom: Same with Charon. Centered on the Anti-Pluto point

Our processing on the profiles presented in figure 1 applies a high-pass filter to better display the roughness we discuss in Figure 2. We also smooth out the pixel-to-pixel noise that occurs due to the scanning geometry of our limb picking technique.

Topography from these limb profiles can be used to compare features such as faults to mathematical models [10]. However, below we focus on the roughness of topography as a function of wavelength, useful for geophysical applications [8].

**Topographic Variance Spectra:** A typical way of expressing the wavelength dependence of surface roughness is through a variance spectrum [11]. After processing the profiles by detrending and interpolating onto a constant spacing, we take the discrete Fourier transform to determine the variance [12]. Figure 2 below shows the resulting variance spectra for Pluto and Charon.

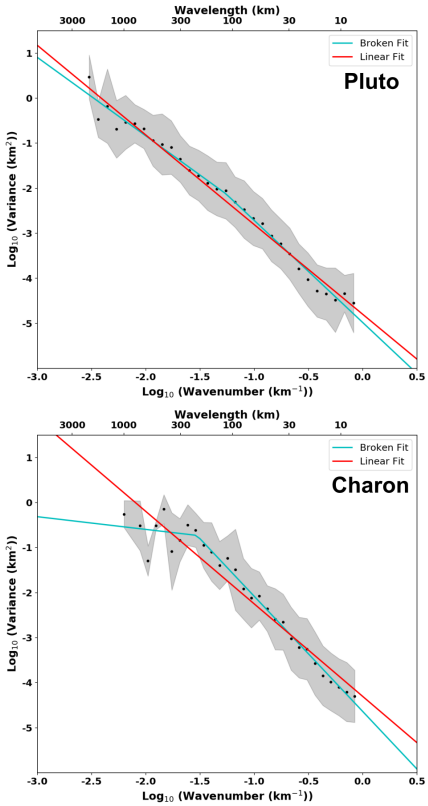


**Figure 2:** Binned topographic variance spectra based on limb profile topography data. Each black point represents the mean in each wavenumber bin, while the shaded region is the standard deviation within a bin. The lines are different fits, red a linear fit and blue a fit that includes a break in slope [13].

Pluto's variance spectrum shows a roughly -2 slope commonly found on other icy bodies [8]. Charon's spectrum shows a similar slope at short wavelengths, but has a shallower slope at long wavelengths. The most statistically significant breakpoint [13] lies at a wavelength of ~200 km.

**Break in Slope Interpretation:** This break in slope at ~200 km likely represents the characteristic flexural parameter for Charon's crust [8]. The flexural parameter relates to the elastic thickness (*Te*) [14]. The solution for *Te* given the break-point wavelength and reasonable parameters results in a value of ~25 km. A more precise approach calculates the expected compensation factor ($F_l$) of the topography due to elastic and membrane stresses (eq. 1). We calculate $C_l$ from [15] equation (27) with and without membrane support.

$$F_l = \frac{1}{1 + \frac{\rho_c}{\rho_m - \rho_c} C_l} \quad (1)$$

where $\rho_c$ is the density of the crust and $\rho_m$ is the density of the mantle.

The results of applying eq (1) are compared with the observations in Figure 3. Pluto requires *Te* >40 km to explain the lack of a break in slope, even with membrane support. Conversely, Charon requires a *Te* ~20±10 km to explain the break in slope, with a better match occurring if membrane stresses are neglected

With these *Te* values, we can constrain the surface heat flux at the time the topography was established [16]. For Pluto the lower bound on *Te* of 40 km is more constraining than a previous bound [10] and is fully consistent with the expected radiogenic heat flux of a few $mWm^{-2}$; it is not consistent with a heat flux estimate derived from an apparently relaxed impact crater [16]. The Charon elastic thickness implies a heat flux of ~30±10 $mWm^{-2}$, which is not consistent with the expected radiogenic heat fluxes and may indicate an extra early heat source, likely the Charon-forming impact.

**Acknowledgments:** Spacecraft data and images were obtained from the PDS Small Bodies Node.

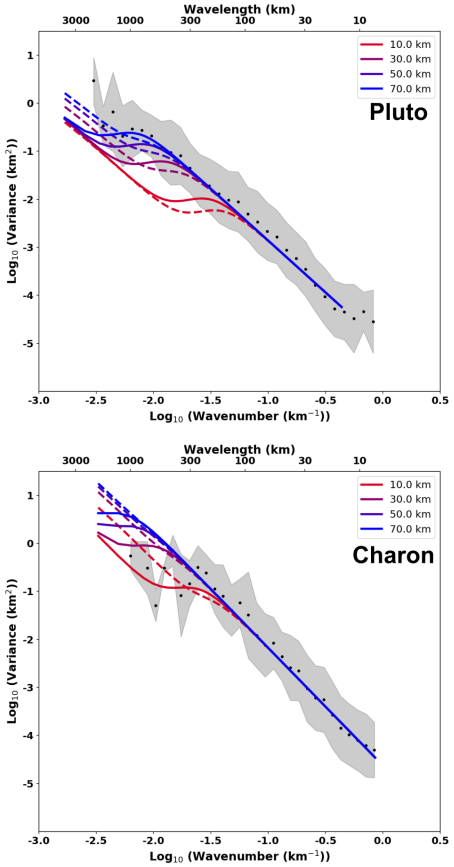


**Figure 3:** Observed variance spectra and modeled variance spectra for two different geophysical considerations. Lines for both models become bluer in hue as *Te* increases. The solid lines are the results for a model that does not include membrane support of topography. The dashed line are results for the model that does include membrane support.

**References:** [1] Stern S. A. et al. (2015) *Science., 350, 6258.* [2] Grundy W. M. et al. (2016) *Science., 351, 6279.* [3] Moore J. M. et al. (2016) ) *Science., 351, 6279.* [4] Beyer R. A. et al. (2017) *Icarus, 287, 161-174.* [5] Schenk P. M. et al. (2018) *Icarus, 314, 400-433* [6] Schenk P. M. et al. (2018) *Icarus, 315, 124-145* [7] Nimmo F. et al. (2017) *Icarus, 287, 12-29.* [8] Nimmo F. et al. (2011) *JGR: Planets 116, E11.* [9] Snyder J. P. (1987) *USGS Report, 1395.* [10] Conrad J. W. et al. (2019) *Icarus, 328, 210-217.* [11] Shepard M. K. et al. (2001) *Geo. Phys. Res.: Planets, 106, 32777-32795.* [12] Press W. H. et al. (1992) *Cambridge University Press.* [13] Main et al. (1999) *GRL, 26, 2801-2804.* [14] Turcotte D. L. and Schubert G. (2014) *Cambridge University Press.* [15] Turcotte D. L. et al. (1981) *JGR: Solid Earth, 86, 3951-3959.* [16] Nimmo F. and McKinnon W. B. (2020) *Univ. Ariz. Press, submitted.*